Original Manuscript

Journal of Vibration and Control
2023, Vol. 0(0) 1–19

DOI: 10.1177/10775463231212530
journals.sagepub.com/home/jvc

Adaptive sliding mode attitude control of 2-degrees-of-freedom helicopter system with actuator saturation and disturbances

Ruobing Li[1], Changyi Lei[2], Baiyang Shi[1], Quanmin Zhu[1], and Xicai Yue[1]

Abstract

The modelling uncertainties, external disturbance and actuator saturation issues will degrade the performance and even the safety of flight. To improve control performance, this study proposes an adaptive U-model based double sliding control (UDSMC) algorithm combined with a radial basis function neural network (RBFNN) for a nonlinear two-degrees-of-freedom (2-DOF) helicopter system. Firstly, the adaptive RBFNN is designed to approximate the system dynamics with unknown uncertainties. Furthermore, two adaptive laws are designed to deal with unknown external disturbances and actuator saturation errors. The global stability of the proposed helicopter control system is rigorously guaranteed by the Lyapunov stability analysis, realizing precise attitude tracking control. Finally, the comparative experiments with conventional SMC and adaptive SMC algorithms conducted on the Quanser Aero2 platform demonstrate the effectiveness and feasibility of the proposed 2-DOF helicopter control algorithm.

Keywords

Two-degrees-of-freedom helicopter, sliding mode control, adaptive neural network, actuator saturation

1. Introduction

A helicopter is a type of vertical take-off and landing (VTOL) aircraft that offers greater hover stability and manoeuvrability than traditional fixed-wing aircraft. Due to its simpler take-off conditions and decent payload capacity, helicopter UAVs are attracting more and more attention from both industry and academia due to their wide range of applications in civil and military areas, including aerial photography, search and rescue missions (Li et al., 2023; Zhao et al., 2022b; Kim and Ahn, 2021). However, complex weather conditions and unpredicted changes in obstacles will affect the effectiveness and stability of the helicopter in actual flight missions, so the accuracy and robustness of the helicopter flight controller are crucial.

The control system design of a two-degree-of-freedom helicopter unmanned aerial vehicle (UAV) has a variety of challenging problems, including firmly couplings, highly nonlinear multi-input multi-output (MIMO) systems, internal parameter uncertainties, external environmental disturbances and actuator output saturation (Wu et al., 2022a; Sadala and Patre, 2018; Zhao et al., 2022a). To overcome these challenges, various control methods have been proposed for the control system design of helicopters, such as state feedback control (Kim and Yoo, 2021], proportional-integral-derivative (PID) based control (Garcia et al., 2012) and linear quadratic regulator (LQR) (Nkemdirim et al., 2022). However, these control techniques have limited performance against internal unmodelled dynamics and external environmental disturbances, and their control requires adaptive and robust control methods to achieve satisfactory performance. To overcome these limitations, sliding mode control (SMC) is proposed and considered to be an effective control method (Utkin et al., 2017; Shtessel and Edwards 2014). Once the sliding surface is reached, unmodelled dynamics, complex nonlinearity and external disturbances will not affect the system, so SMC has strong robustness. Accordingly, SMC method has been received a lot of research (Yang and Niu, 2023; Ye et al.,

[1]School of Engineering, University of the West of England-Frenchy Campus, Coldharbour Lane Bristol, UK
[2]King's College London, London, UK

Received: 31 May 2023; accepted: 19 October 2023

Corresponding author:
Ruobing Li, School of Engineering, University of the West of England-Frenchy Campus, 11 jekyll Close, Stoke Gifford, Coldharbour Lane Bristol BS16 1UX, UK.
Email: ruobing2.Li@live.uwe.ac.uk

2022; Inomoto et al., 2022; Fei et al., 2022), which has been also applied into real-time industrial applications to deal with complex mechanical control issues effectively (Ahmed et al., 2022, 2022b; Dong et al., 2022; Zhang et al., 2023).

In recent years, numerous studies have introduced the application of SMC technology for 2-DOF helicopter attitude control, including the high-order sliding mode control of optimal attitude tracking control (Humaidi and Hasan, 2019), which combines high-order sliding mode technology and LQR and solves the identified problems of the system. Helicopter active fault-tolerant sliding mode controller for sensor faults, combined with fuzzy logic, real-time estimation of sensor faults and control system input compensation (Wang et al., 2020), learning-based helicopter trajectory tracking sliding mode control (Reyhanoglu et al., 2022; Zhang and Xian, 2021), etc. Although SMC can deal with system uncertainties and disturbances effectively, but their upper bounds must be known. However, it is usually difficult to obtain an accurate upper bound of disturbance in actual control. Therefore, adaptive SMC can be used to solve the problem that the upper limit of error interference is unknown. Recently, adaptive SMC has been received a lot of research, such as RBFNN based adaptive SMC (Feng et al., 2022), barrier function based adaptive SMC (Shao et al., 2022), adaptive SMC with hysteresis compensation-based neuroevolutionary (Son et al., 2022) and hybrid robust adaptive SMC (Milbradt et al., 2023). Zou et al. (2022) designed an adaptive second-order sliding mode observer to compensate for time-varying lumped disturbances, and proves finite-time global stability through Lyapunov stability theory. At the same time, the efficient nonlinear estimation and fitting characteristics of the neural network (NN) are widely used to deal with uncertain dynamic characteristics in the system model (Abiodun et al., 2018; He et al., 2015). The helicopter attitude sliding mode control algorithm with specified performance is designed using the neural network, and the NN estimation system is used. Unmodelled dynamics (Wu et al., 2022b), an adaptive neural network based fault-tolerant control method for 3-DOF helicopter systems is proposed to deal with unknown system modelling uncertainties, disturbances and actuator failures (Mokhtari et al., 2021), fast terminal sliding mode attitude tracking control for 2-DOF helicopter systems with an adaptive input compensation was proposed in Shen and Xu (2021), which solves the problem of input and output constraints of the helicopter system.

However, these works did not take into account the saturation effect of helicopter actuators. In order to protect the machine, actuator saturation (Zhu et al., 2011; Li and Lin, 2018; Bu et al., 2022) widely exists in practical industry control systems including helicopter control system. If it is not considered in the control system design, this will lead to poor flight performance of the helicopter, and the controller may even 'kill' the torque output of the actuator. Therefore, amount of advanced control algorithms have been proposed and developed to solve the actuator saturation problem. Ghaffari et al. (2022) introduced composite nonlinear feedback (CNF), combined with the super-twist sliding mode control method, to try to solve the problem of helicopter actuator saturation. In Zhu et al. (2023), a dual-loop control quadrotor position control algorithm based on conventional PID algorithm is proposed to deal with system state errors and actuator constraints. In the article (Guo et al., 2020), a control algorithm based on reverse thrust control that can stabilize a UAV with actuator saturation is proposed. Feng et al. used the radial basis function neural network (RBFNN) to compensate the helicopter system input saturation errors, but this study did not consider external disturbances. According to the above, although the research on the UAV control algorithm with system actuator output saturation has made great progress, the related research considering both control input saturation and disturbances is still not satisfying enough due to its unpredicted disturbances, complex nonlinear and strong coupling problems.

Meanwhile, the switching function used in the sliding mode algorithm leads to the ubiquitous chattering problems (Wu et al., 2022c; Feng et al., 2014; Wan et al., 2020; Soon et al.,2022), which together with unknown uncertainties and disturbances, actuator saturation, limit the real-time applications of sliding mode control in industry such as helicopters. To address these limitations, an adaptive control algorithm is proposed in this paper to develop an adaptive 2-DOF helicopter attitude control scheme with three update laws through the U-model-based adaptive dual sliding mode control (UDSMC) (Zhu et al., 2022) method and RBFNN, the first adaptive law is built for unknown unmodelled dynamics, the second adaptive solves the helicopter actuator saturation, and the last one is constructed for the unknown upper limit of external disturbances of the system. At the same time, the double-layer sliding structure of UDSMC effectively reduces the system vibration and improves the steady-state performance of the system. In summary, this study makes the following three main contributions.

(1) Considering the unknown dynamics of the system, external environment disturbance and actuator saturation, an adaptive NN based control algorithm using the UDSMC is designed for a 2-DOF helicopter, and the stability of its closed-loop system is established through Lyapunov stability analysis.
(2) The proposed control scheme consists of a decoupling algorithm, a baseline invariant controller to achieve the desired control performance, a DSMC-based dynamic inverter to achieve nonlinear dynamic cancellation and robustness and three adaptive laws to solve system control inputs saturation errors, external disturbances and NN approximated errors, which are well established in developing controllers without requirements

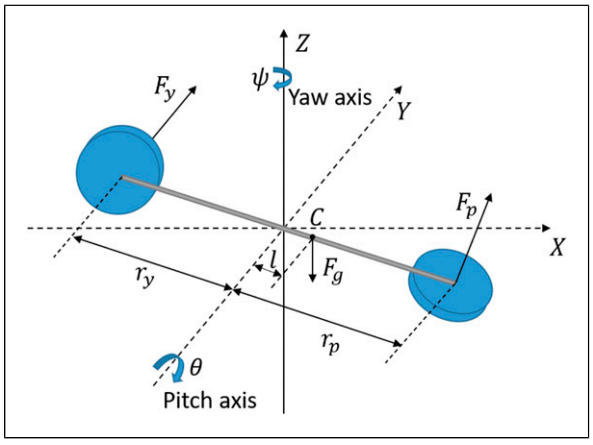

Figure 1. 2-DOF helicopter framework.

of precise parameters and known upper boundary of the lumped disturbances.

(3) To illustrate the superiority of the proposed control algorithm, we compare it with the conventional SMC and adaptive SMC (Zou et al., 2022) methods under different scenarios.

The organization of the rest sections are as follows: Section 2 discusses the dynamics modelling and control problems of a 2-DOF helicopter. Section 3 introduces the decoupling algorithm, extended MIMO UDSMC algorithm and the design procedure of the 2-DOF helicopter system, and its global stability is analyzed by Lyapunov stability theory. Section 4 sets up two experiments and discusses the comparative experimental simulation results between the proposed adaptive UDSMC, the conventional SMC and adaptive SMC (Zou et al., 2022) methods. Section 5 concludes this research.

2. Problem statement and preliminaries

2.1. Model of two-degrees-of-freedom helicopter system

Figure 1 shows the structure of a 2-DOF helicopter system (Reyhanoglu et al., 2022), where C presents centre of mass, and l is the length from the pitch axis to the centre of mass of the helicopter body. Yaw and pitch motions are controlled by the F_y and F_p thrust forces, respectively. The following kinematic model for the 2-DOF helicopter derived by the Euler-Lagrange formula can be therefore obtained as (Reyhanoglu et al., 2022):

$$\begin{cases} (J_p + ml^2)\ddot{\theta} = k_{p1}u_p + k_{p2}u_y - B_p\dot{\theta} - ml^2 sin(\theta)cos(\theta)\dot{\psi}^2 \\ \quad - mlgcos(\theta) \\ (J_y + ml^2 cos^2(\theta))\ddot{\psi} = k_{y1}u_p + k_{y2}u_y - B_y\dot{\psi} \\ \quad +2ml^2\dot{\theta}sin(\theta)cos(\theta)\dot{\psi} \end{cases} \tag{1}$$

where θ and ψ are pitch and yaw angles, m is the total mass of the helicopter, g is the gravitational acceleration. J_p and J_y are the moment of inertia for pitch and yaw axis, respectively. u_p and u_y are the control inputs to pitch and yaw motors. k_{p1}, k_{p2}, k_{y1} and k_{y2} are their thrust force constants. For simplification, system (1) can be rewritten as

$$\begin{cases} (J_p + ml^2)\ddot{\theta} = k_{p1}u_p + k_{p2}u_y + \Gamma \\ (J_y + ml^2 cos^2(\theta))\ddot{\psi} = k_{y1}u_p + k_{y2}u_y + \mathbb{N} \end{cases} \tag{2}$$

where $\Gamma = -B_p\dot{\theta} - ml^2 sin(\theta)cos(\theta)\dot{\psi}^2 - mlgcos(\theta)$ and $\mathbb{N} = -B_y\dot{\psi} + 2ml^2\dot{\theta}sin(\theta)cos(\theta)\dot{\psi}$ absorb all dynamics for pitch and yaw motor with B_p and B_y being the pitch and yaw viscous friction constant. Consider about complex and unpredicted environment and internal modelling uncertainties, introducing modelling errors and external disturbances to model described in (2) as

$$\begin{cases} \ddot{\theta} = \dfrac{k_{p1}u_p + k_{p2}u_y + \Gamma + \Delta\Gamma}{(J_p + ml^2)} + d_p \\ \ddot{\psi} = \dfrac{k_{y1}u_p + k_{y2}u_y + \mathbb{N} + \Delta\mathbb{N}}{(J_y + ml^2 cos^2(\theta))} + d_y \end{cases} \tag{3}$$

where $\Delta\Gamma$ is model uncertainty of Γ, d_p is external disturbance in pitch motor. $\Delta\mathbb{N}$ is model uncertainty of $\mathbb{N}$ and d_y is external disturbance in yaw motor. In practical flight environment, model-matched system is hard to obtain due to the time-varying environment. Therefore, introducing model uncertainties $\Delta\Gamma$ and $\Delta\mathbb{N}$ and external disturbances d_p and d_y are reasonable.

Assumption 1. The external disturbance d_p and d_y are smooth and bounded as $d_p \le \overline{d}_p$ and $d_y \le \overline{d}_y$ with $\overline{d}_p$ and $\overline{d}_y$ represent unknown positive constant.

2.2. Actuator saturation

The 2-DOF helicopter equips with two motors, and each motor will have saturation phenomenon because of physical limitations. Consequently, the relation of actual/saturated control input $sat(u_i)$ and ideal control input u_i can be described as:

$$sat(u_i) = \begin{cases} u_{max}, u_i > u_{max} \\ u_i, |u_i| \le u_{max}, \ i \in R^+ \\ -u_{max}, u_i < -u_{max} \end{cases} \tag{4}$$

where u_{max} is the threshold/saturation for control input. Accordingly, the control input above such threshold will be restricted as u_{max}.

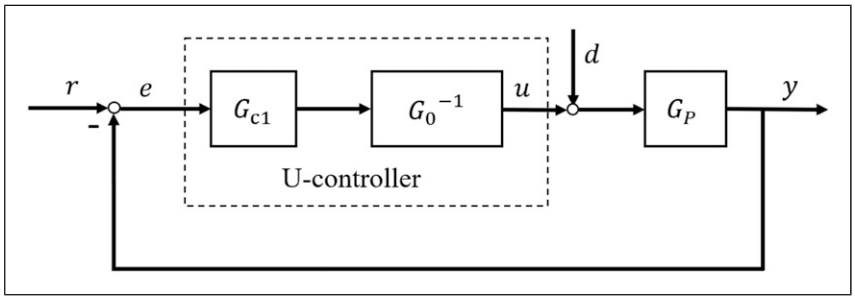

Figure 2. U-model based control system design framework.

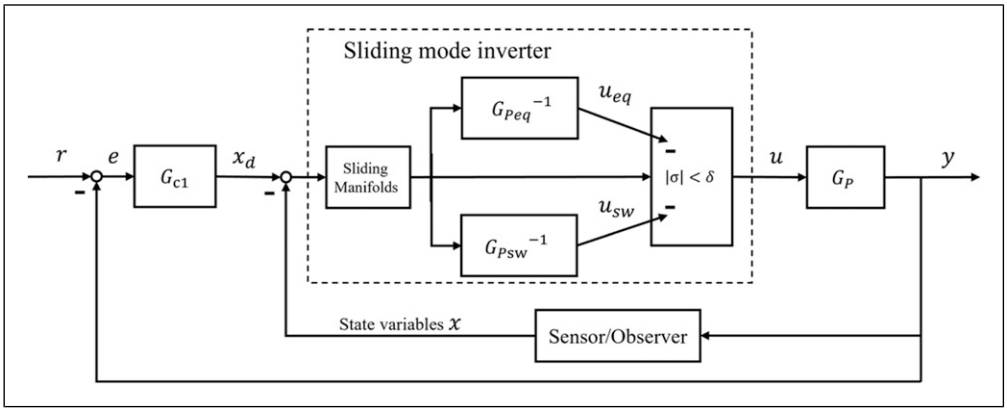

Figure 3. Design framework of UDSMC.

3. Controller design

3.1. U-model based control

The U-model based control (U-control) enables the inversion of the controlled plant and the design of the baseline controller in dual feedback loops. The framework of the continuous-time (CT) U-control system (Li et al., 2020) is depicted in Figure 2. In U-control, the inner loop is the dynamic inversion design of the plant to nullify the system nonlinearities and dynamics (Li et al., 2021a, 2022). This process converts the controlled plant into an identity matrix or unit constant combined with its inversion. Subsequently, the output of the U-control system is obtained as follows:

$$y = \frac{G_{c1}G_0^{-1}G_P}{1 + G_{c1}G_0^{-1}G_P}r + \frac{G_P}{1 + G_{c1}G_0^{-1}G_P}d \tag{5}$$

where G_{c1} is a baseline invariant controller, G_P represents the controlled plant, G_0^{-1} is its nominal dynamic inversion and r is the desired tracking signal. When the controlled plant is perfectly modelled and there is no system external disturbance, the model G_P equals G_0, and as a result, system output (5) can be simplified as:

$$y = \frac{G_{c1}}{1 + G_{c1}}r = Gr \tag{6}$$

Specifically, G represents the closed-loop gain for control system, which can be customized and fine-tuned based on various damping ratios (denoted by ζ) and natural frequencies (denoted by ω_n) of the linear invariant controller, G_{c1}.

Remark 1. The application of inversion necessitates the controlled plant to be Bounded Input and Bounded Output (BIBO) stable and to have no unstable zero dynamics. Upon solving for the highest-order derivatives of the system input $u^{(m)}$, the other u-related derivatives can be derived through the integral operation of $u^{(m)}$.

3.2. U-model based double sliding control

In Section 3.1, the fundamental concept of the U-control system is presented (Li et al., 2020). The original U-inverter is sensitive to the precision of the system model, which can lead to less-than-optimal control performance in real-time control applications (Li et al., 2021b). To overcome this issue, UDSMC adopts the DSMC approach to obtain a robust dynamic inverter G_0^{-1}. UDSMC's design framework is shown in Figure 3, which contains two closed-loop subsystems: (1) the sliding mode inverter in the inner loop is designed by DSMC, aiming to cancel the system dynamics and maintain robustness, that is, achieve $G_0^{-1}G_P = 1$; and (2) The invariant controller G_{c1} in the external loop is designed to achieve specified control

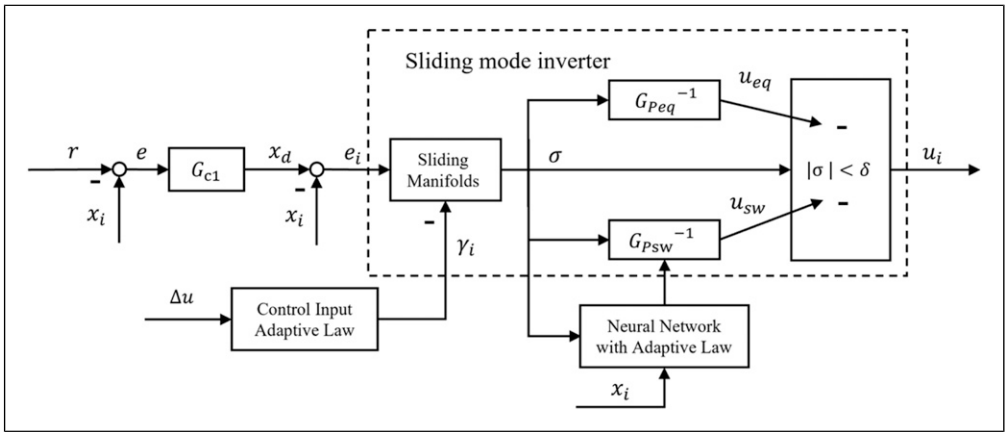

Figure 4. Adaptive UDSMC framework.

performance. Accordingly, the UDSMC design procedures are listed following.

(1) Design a global sliding surface, denoted as σ_g, that characterizes the desired performance of the system when it remains on the sliding mode (SM). The global sliding surface has a boundary δ within the SM interval and is designed as $\sigma_{ig} = \sigma_i + \delta_i, 0 \le |\delta_i| \le \delta$ with $\sigma_i = c_i e_i + \dot{e}_i$ being the classical sliding surface function, c_i being the sliding coefficient.

(2) Design a switching controller u_{sw} to steer the system states towards the sliding band in a finite time and maintain the system state motion on the band thereafter. Let $\dot{\sigma}_{ig} = f_g + f_u u_{sw}$ with f_g representing all the neglected bounded terms in a classical SMC design, which yields as $u_{sw} = -k_g \mathrm{sgn}(S + \delta_1)$ with $k_g \in \mathbb{R}^+$ being a positive gain coefficient and $\mathrm{sgn}(*)$ being the sign function.

(3) Design a local sliding surface σ_l with an equivalent controller u_{eq} to steer the system states towards from the sliding band to the sliding surface in a finite time and maintain the system state motion on the surface thereafter. Let $\sigma_{il} = \sigma_i$ satisfying the classical Hurwitz stability criterion. The derivative of σ_{il}, can be represented as $\dot{\sigma}_{il} = f_l + f_u u_{eq}$, where f_l denotes all the neglected bounded terms in a classical SMC design. The matching condition of $f_l = k_2 \sigma$ must be satisfied, where k_2 represents a bounded unknown tangent factor of σ_i. In such case, it yields as $u_{eq} = -k_l S$. Finally, the DSM controller is designed as $u = u_{eq} + u_{sw}$.

(4) Design an invariant controller G_{c1} such that the overall closed-loop control gain satisfies the user-desired specification by $G = \frac{\omega_n{}^2}{s^2 + 2\zeta\omega_n s + \omega_n{}^2}$, with ζ being the system damping ratio and ω_n being the system undamped natural frequency. Finally, $G_{c1} = \frac{G}{1-G}$.

Remark 2. It should be emphasized that the dynamic inversion of the controlled plant should exist and satisfy the globally consistent Lipschitz continuity (Zhu et al., 2022): $\|G(x_1) - G(x_2)\| \le \gamma_1 G \|x_1 - x_2\|, \forall x_1, x_2 \in \mathbb{R}^n$ and $\|G^{-1}(x_1) - G^{-1}(x_2)\| \le \gamma_2 G^{-1} \|x_1 - x_2\|, \forall x_1, x_2 \in \mathbb{R}^n$.

3.3. Model transformation

Let $x_1 = \theta$, $x_2 = \dot{\theta}$, $x_3 = \psi$ and $x_4 = \dot{\psi}$, then (3) can be rewritten as

$$\begin{cases} \dot{x}_1 = x_2 \\ \dot{x}_2 = \dfrac{k_{p1}u_p + k_{p2}u_y + \Gamma + \Delta\Gamma}{J_p + ml^2} + d_p \\ \dot{x}_3 = x_4 \\ \dot{x}_4 = \dfrac{k_{y1}u_p + k_{y2}u_y + \mathbb{N} + \Delta\mathbb{N}}{J_y + ml^2 \cos^2(\theta)} + d_y \end{cases} \tag{7}$$

Choose desired tracking signal as θ_d and ψ_d, let $e_1 = x_1 - \theta_d$, $e_2 = \dot{x}_1 - \dot{\theta}_d$, $e_3 = x_3 - \psi_d$ and $e_4 = \dot{x}_3 - \dot{\psi}_d$ with θ_d and ψ_d being the desired pitch and yaw angles, respectively, and $\dot{\theta}_d$ and $\dot{\psi}_d$ being the pitch and yaw angular speeds, respectively. Then (7) can be rewritten as error tracking system

$$\begin{cases} \dot{e}_1 = e_2 \\ \dot{e}_2 = \dfrac{k_{p1}u_p + k_{p2}u_y + \Gamma + \Delta\Gamma}{J_p + ml^2} + d_p - \ddot{\theta}_d \\ \dot{e}_3 = e_4 \\ \dot{e}_4 = \dfrac{k_{y1}u_p + k_{y2}u_y + \mathbb{N} + \Delta\mathbb{N}}{J_y + ml^2 \cos^2(\theta)} + d_y - \ddot{\psi}_d \end{cases} \tag{8}$$

Assumption 2. In this study, the trajectory x_d is expected to be continuously bounded and derivable.

For simplification, equations (7) and (8) can be rewritten as

$$\begin{cases} \dot{X}_1 = X_2 \\ \dot{X}_2 = F(X) + G(X)U + D \end{cases} \tag{9}$$

$$\begin{cases} \dot{E}_1 = E_2 \\ \dot{E}_2 = F(X) + G(X)U + D - R \end{cases} \tag{10}$$

where $X_1 = [\theta, \psi]^T$, $X_2 = [\dot{\theta}, \dot{\psi}]^T$, $U = [u_p, u_y]^T$, $F(X) = \left[\frac{\Gamma}{J_p+ml^2}, \frac{\mathbb{N}}{J_y+ml^2\cos^2(\theta)}\right]^T$,

$$D = \left[\frac{\Delta\Gamma}{J_p+ml^2} + d_p, \frac{\Delta\mathbb{N}}{J_y+ml^2\cos^2(\theta)} + d_y\right]^T,$$

$$G(X) = \begin{bmatrix} \frac{k_{p1}}{J_p+ml^2} & \frac{k_{p2}}{J_p+ml^2} \\ \frac{k_{y1}}{J_y+ml^2\cos^2(\theta)} & \frac{k_{y2}}{J_y+ml^2\cos^2(\theta)} \end{bmatrix},$$

$R = \left[\ddot{\theta}_d, \ \ddot{\psi}_d\right]^T$.

For decoupling of system (7), let $\dot{E}_2 = G(X)U$, then control inputs can be designed as:

$$U = G(X)^{-1}\begin{bmatrix} v_1 \\ v_2 \end{bmatrix} \tag{11}$$

Substituting above conversion into equation (11), it becomes

$$\begin{cases} \dot{E}_1 = E_2 \\ \dot{E}_2 = F(X) + \begin{bmatrix} v_1 \\ v_2 \end{bmatrix} + D - R \end{cases} \tag{12}$$

In such case, the coupling system presented in (7) can be converted into decoupling system in (12).

3.4. Adaptive inverter design

According to Section 3.2, it can be observed that the upper boundaries of system neglected terms (including system dynamics and disturbances) are required for controller design, which is hard to obtain in practical application control system. Additionally, overestimating such boundaries can lead to excessive controller gains, resulting in chattering and control inputs saturation issues. Therefore, this section proposes an adaptive DSM inverter using RBFNN to estimate/approximate the system dynamics and three adaptive laws to solve the problems caused by external system disturbances and control input saturation. The adaptive UDSMC framework is shown in Figure 4, where x_i indicates the system state variables, Δu is the error between the ideal control input and actual control input.

Comparing Figures 4 and 3, the sliding mode inverter presented in dashed area is not changed. However, NN and control input auxiliary system with adaptive law are introduced into UDSMC system to update the control gain and the design of sliding surface described in Section 3.2. To illustrate such adaptive UDSMC design principles, define the unknown functions as $\mathcal{F}_1 = \frac{\Gamma+\Delta\Gamma}{J_p+ml^2} - \ddot{\theta}_d$ and $\mathcal{F}_2 = \frac{\mathbb{N}+\Delta\mathbb{N}}{J_y+ml^2\cos^2(\theta)} - \ddot{\psi}_d$. Since Γ and $\mathbb{N}$ are not precise with modelling uncertainties, $\Delta\Gamma$ and $\Delta\mathbb{N}$ are unknown, by introducing the Neural Network (NN), $\mathcal{F}_i$ can be approximated by

$$\mathcal{F}_i = W_i^T H_i(X) + \varepsilon_i \tag{13}$$

where X is the input of the NN. W_i represents the optimal weight vector, ε_i is NN compensation error and $|\varepsilon_i| \le \bar{\varepsilon}_i$ with $\bar{\varepsilon}_i$ being small unknown positive constants. $H_i(X) = [h_{i,1}(X), h_{i,2}(X), \cdots, h_{i,n}(X)]^T$ denotes the radial basis vector and $h_{i,j}(X)$ is given by

$$h_{i,j}(X) = \exp\left(-\frac{\|X - c_{i,j}\|_2^2}{b_j^2}\right) with j = 1, 2, \cdots, n \tag{14}$$

where j is the number of nodes in the hidden layer of the network. Then the error system can be converted into

$$\begin{cases} \dot{E}_1 = E_2 \\ \dot{E}_2 = \mathcal{F} + \begin{bmatrix} v_1 \\ v_2 \end{bmatrix} + D - R \end{cases} \tag{15}$$

where $\mathcal{F} = [\mathcal{F}_1, \mathcal{F}_2]^T$, with $\mathcal{F}_1 = W_1^T H_1(X) + \varepsilon_1$ and $\mathcal{F}_2 = W_2^T H_2(X) + \varepsilon_2$.

Then design the first adaptive controller auxiliary law for control inputs saturation as:

$$\dot{\gamma} = A\gamma + B\Delta u \tag{16}$$

where $A = \begin{bmatrix} -\rho_i & 1 \\ 0 & -\rho_{i+1} \end{bmatrix}$ with ρ_i being positive constant, $B = \begin{bmatrix} 0 \\ 1 \end{bmatrix}$, $\Delta u_i = sat(u_i) - u_i$ are the error between actual control inputs and desired control inputs. Let $e_1 = x_1 - \theta_d - \gamma_1$, $\dot{e}_1 = \dot{x}_1 - \dot{\theta}_d - \dot{\gamma}_1$, $e_3 = x_3 - \psi_d - \gamma_3$ and $\dot{e}_3 = \dot{x}_3 - \dot{\psi}_d - \dot{\gamma}_3$, then the global sliding surface described in Section 3.2 can be designed as

$$\sigma_{ig} = c_i e_i + \dot{e}_i + \delta_i with c \in R^+, i = 1, 3 \tag{17}$$

Accordingly, the derivative of equation (17) can be calculated as

$$\begin{aligned} \dot{\sigma}_{ig} &= c_i\dot{e}_i + \ddot{e}_i = c\dot{e}_i + v_i + W_i^T H_i(X) + \varepsilon_i + D_i - \ddot{\gamma}_i \\ &= c\dot{e}_i + v_i + W_i^T H_i(X) + \varepsilon_i + D_i + \rho_i\dot{\gamma}_i - \dot{\gamma}_{i+1} \\ &= c\dot{e}_i + v_i + W_i^T H_i(X) + \varepsilon_i + D_i + \rho_i(-\rho_i\gamma_i + \gamma_{i+1}) \\ &\quad -(-\rho_{i+1}\gamma_{i+1} + \Delta u_i) = c\dot{e}_i + v_i + W_i^T H_i(X) + \varepsilon_i + D_i \\ &\quad + \rho_i(-\rho_i\gamma_i + \gamma_{i+1}) + \rho_{i+1}\gamma_{i+1} = c\dot{e}_i + v_i + W_i^T H_i(X) \\ &\quad + \varepsilon_i + D_i + \varkappa_i \end{aligned} \tag{18}$$

where $\varkappa_i = \rho_i(-\rho_i\gamma_i + \gamma_{i+1}) + \rho_{i+1}\gamma_{i+1}$. Define $\lambda_i = \bar{\varepsilon}_i + \overline{D}_i$, then $\lambda_i \ge |\varepsilon_i + D_i|$. Choose global candidate Lyapunov function as

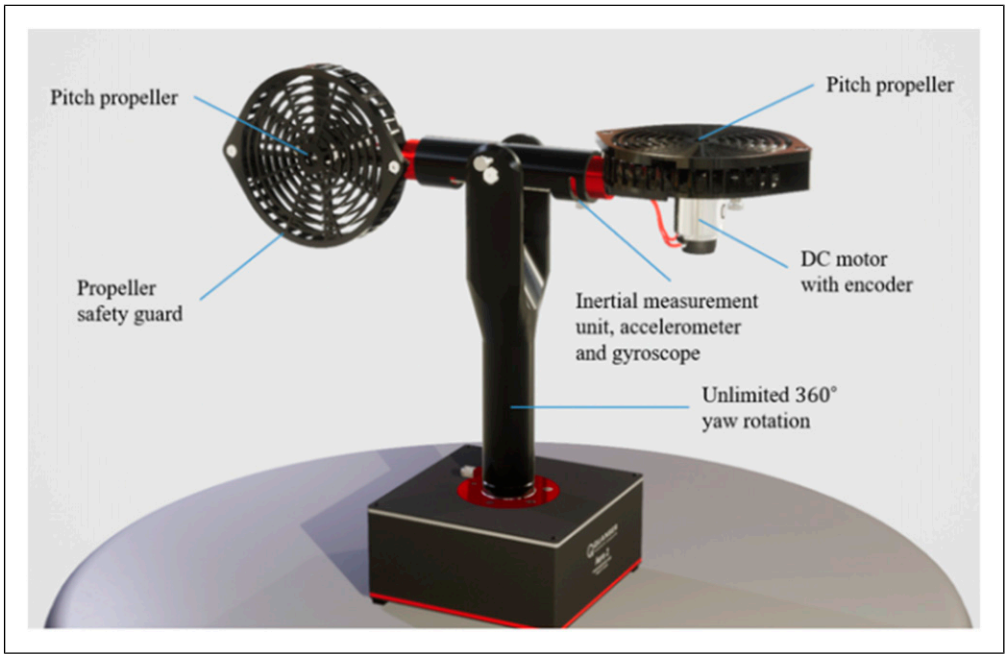

Figure 5. Quanser Aero2 experimental platform.

$$V_{ig} = \frac{1}{2}\sigma_{ig}^2 + \frac{1}{2}\tilde{W}_i^T \hat{W}_i + \frac{1}{2}\tilde{\lambda}_i^2 \tag{19}$$

Also, the local candidate Lyapunov function is chosen as

$$V_{il} = \frac{1}{2}\sigma_{il}^2 = \frac{1}{2}\sigma_i^2 \tag{20}$$

where $\tilde{W}_i = \hat{W}_i - W_i$ and $\tilde{\lambda}_i = \hat{\lambda}_i - \lambda_i$ with $\hat{W}_i$ and $\hat{\lambda}_i$ being predicted values of W_i and λ_i, respectively. Taking the derivative of Lyapunov function in equation (19), we obtain

$$\begin{aligned}
\dot{V}_{ig} &= \dot{\sigma}_{ig}\sigma_{ig} + \tilde{W}_i^T \dot{\hat{W}}_i + \dot{\tilde{\lambda}}_i \hat{\lambda}_i \\
&= \left(c_i \dot{e}_i + v_i + \left(\hat{W}_i^T - \tilde{W}_i^T\right) H_i(X) + \varepsilon_i + D_i + \varkappa_i\right)\sigma_{ig} \\
&+ \tilde{W}_i^T \dot{\hat{W}}_i + \tilde{\lambda}_i \dot{\hat{\lambda}}_i = \left(c_i \dot{e}_i + v_i + \hat{W}_i^T H_i(X) + \varepsilon_i + D_i + \varkappa_i\right)\sigma_{ig} \\
&+ \tilde{W}_i^T \dot{\hat{W}}_i + \tilde{\lambda}_i \dot{\hat{\lambda}}_i - \tilde{W}_i^T H_i(X)\sigma_{ig} \\
&= \Big(c_i \dot{e}_i + v_i + \hat{W}_i^T H_i(X) \\
&+ \varepsilon_i + D_i + \varkappa_i\Big)\sigma_{ig} \\
&+ \tilde{W}_i^T \left(\dot{\hat{W}}_i - H_i(X)\sigma_i\right) + \tilde{\lambda}_i \dot{\hat{\lambda}}_i
\end{aligned} \tag{21}$$

Design the second NN approximated adaptive law for system dynamics and modelling uncertainties as

$$\dot{\hat{W}}_i = H_i(X)\sigma_i \tag{22}$$

Substituting equation (22) into equation (21), it has

$$\dot{V}_{ig} = \left(c_i \dot{e}_i + v_i + \hat{W}_i^T H_i(X) + \varepsilon_i + D_i + \varkappa_i\right)\sigma_{ig} + \tilde{\lambda}_i \dot{\hat{\lambda}}_i \tag{23}$$

Then introduce an accessorial variable as

$$\mu_i = c_i \dot{e}_i + \hat{W}_i^T H_i(X) + \hat{\lambda}_i sgn(\sigma_{ig}) + \varkappa_i \tag{24}$$

Substituting equation (24) into equation (23), it has

$$\begin{aligned}
\dot{V}_{ig} &= \left(\mu_i - k_{l,i}\sigma_{ig} + v_i + \varepsilon_i + D_i\right)\sigma_{ig} + \tilde{\lambda}_i \dot{\hat{\lambda}}_i \\
&= \sigma_{ig}(\mu_i + v_i) + \sigma_{ig}\left(-\hat{\lambda}_i sgn(\sigma_{ig}) + \varepsilon_i + D_i\right) + \tilde{\lambda}_i \dot{\hat{\lambda}}_i \\
&= \sigma_{ig}(\mu_i + v_i) + \left(-\lambda_i |\sigma_{ig}| + \sigma_{ig}(\varepsilon_i + D_i)\right) \\
&+ \tilde{\lambda}_i \left(\dot{\hat{\lambda}}_i - |\sigma_{ig}|\right)
\end{aligned} \tag{25}$$

According to $\lambda_i \geq |\varepsilon_i + D_i|$, the situation $-\lambda_i|\sigma_{ig}| + \sigma_{ig}(\varepsilon_i + D_i) \leq 0$ holds. Then design the third adaptive law for system external disturbances as:

$$\dot{\hat{\lambda}}_i = |\sigma_{ig}| \tag{26}$$

Accordingly, substituting (26) into (25), it has

$$\dot{V}_{ig} \leq \sigma_{ig}(\mu_i + v_i) \tag{27}$$

Then the control inputs are therefore designed as $v_i = -k_{sw,i} sgn(\sigma_{ig}) - k_{eq,i}\sigma_i$, then (27) becomes

$$\dot{V}_{ig} \leq \sigma_{ig}\left(-k_{sw,i} sgn(\sigma_{ig}) + \mu_i\right) \leq -|\sigma_i|\left(k_{eq,i} - \mu_i\right) \tag{28}$$

Then taking the derivative of Lyapunov function (20), it comes

$$\dot{V}_{il} = \dot{\sigma}_i \sigma_i = \left(k_i \sigma_i - k_{eq,i}\sigma_i\right)\sigma_i \leq -|\sigma_i|^2\left(k_{eq,i} - k_i\right) \tag{29}$$

To satisfy $\dot{V}_{ig} < 0$ and $\dot{V}_{il} < 0$ for attitude control stability for helicopter, it comes $k_{sw,i} - \mu_i > 0$ and $k_{eq,i} - k_i$, therefore it comes

$$k_{sw,i} > |\mu_i| \quad \text{and} \quad k_{eq,i} > |k_i| \tag{30}$$

In such case, the stability of control system holds. Substituting $v_i = -k_{sw,i}\text{sgn}(\sigma_{ig}) - k_{eq,i}\sigma_i$ into (11), the actual control inputs can be designed as

$$\begin{bmatrix} u_p \\ u_y \end{bmatrix} = G(X)^{-1} \begin{bmatrix} v_1 \\ v_2 \end{bmatrix} = -\begin{bmatrix} \dfrac{k_{y2}\left(J_p + ml^2\right)}{k_{p1}k_{y2} - k_{p2}k_{y1}} & -\dfrac{k_{p2}\left(J_y + ml^2\cos^2(\theta)\right)}{k_{p1}k_{y2} - k_{p2}k_{y1}} \\ -\dfrac{k_{y1}\left(J_p + ml^2\right)}{k_{p1}k_{y2} - k_{p2}k_{y1}} & \dfrac{k_{p1}\left(J_y + ml^2\cos^2(\theta)\right)}{k_{p1}k_{y2} - k_{p2}k_{y1}} \end{bmatrix} \begin{bmatrix} k_{sw,1}\text{sgn}\left(\sigma_{ig}\right) + k_{eq,1}\sigma_i \\ k_{sw,3}\text{sgn}\left(\sigma_{ig}\right) + k_{eq,3}\sigma_i \end{bmatrix} \tag{31}$$

Remark 3. The modelling uncertainty of the system has been considered in (7) as $\Delta\Gamma$, so the control input coefficient matrix described above is determined. Consider the system described in (7) with the designed controller (31), associated with three proposed adaptive laws described in (16), (22) and (26), the system tracking error will be converged to the origin within finite time.

Remark 4. In this proposed control algorithm, the RBF is established to deal with the uncertain system dynamics; therefore, the precise parameter is not required for controller's design. Also, the upper bounds of the external disturbances caused by complex environment are not required because of the three adaptive laws, thereby avoiding the overestimation of the switching gain. Eventually, the proper switching gain and double-sliding structure reduce the control chattering issue efficiently.

Table 1. 2-DOF helicopter design parameters.

Parameter	Value
J_p	0.0219 kg·m^2
B_p	0.0071 N/V
k_{p1}	0.0011 N•m/V
k_{y1}	−0.0027 N•m/V
L	0.0071 m
sat(u_i)	+/−24 V
J_y	0.022 kg·m^2
B_y	0.022 N/V
k_{p2}	0.0022 N•m/V
k_{y2}	0.0022 N•m/V
m	1.075 kg

4. Experimental simulation

To demonstrate the validity and effectiveness of the proposed control algorithm, comparative experiments of the proposed control system, SMC system and adaptive SMC system are established on a 2-DOF helicopter platform (Quanser Aero2) shown in Figure 5. The specific parameters of the 2-DOF helicopter model are presented in Table 1. The adaptive SMC and conventional SMC design procedures are proposed as follows refers to the paper (Zou et al., 2022).

The compared SMC and adaptive SMC algorithms design procedures are shown as follows. According to model (1), let

$$\begin{aligned} \beta_1 &= J_p + ml^2 \\ \beta_2 &= -B_p\dot{\theta} - ml^2\sin(\theta)\cos(\theta)\dot{\psi}^2 - mlg\cos(\theta) \\ \gamma_1 &= J_y + ml^2\cos^2(\theta) \\ \gamma_2 &= -B_y\dot{\psi} + 2ml^2\dot{\theta}\sin(\theta)\cos(\theta)\dot{\psi} \end{aligned} \tag{32}$$

Then the model (1) can be converted to as follows:

$$\begin{cases} \dot{\mathfrak{X}}_1 = \mathfrak{X}_2 \\ \dot{\mathfrak{X}}_2 = \mathcal{F}(x) + \mathcal{G}(x)u + \mathcal{D} \end{cases} \tag{33}$$

where $\mathfrak{X}_1 = [\theta, \varphi]^T$, $\mathfrak{X}_2 = [\dot{\theta}, \dot{\varphi}]^T$ and $\mathcal{F}(x) = \left[\frac{\beta_2}{\beta_1}, \frac{\gamma_2}{\gamma_1}\right]^T$,

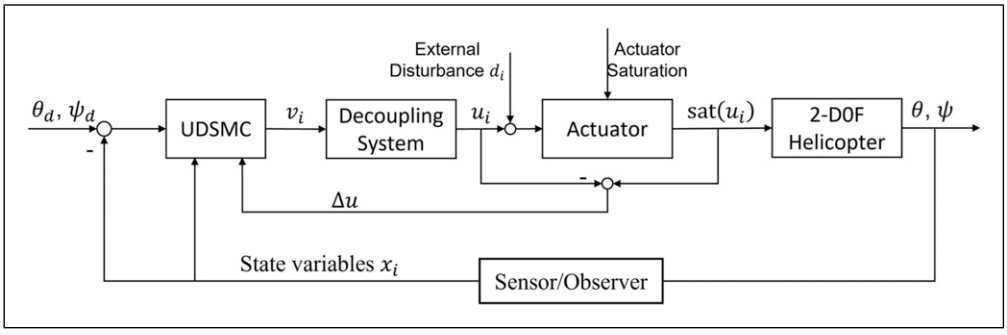

Figure 6. UDSMC control system framework for 2-DOF helicopter.

$\mathcal{G}(x) = \begin{bmatrix} \frac{k_{p1}}{\gamma_1} & \frac{k_{p2}}{\gamma_1} \\ \frac{k_{y1}}{\gamma_1} & \frac{k_{y2}}{\gamma_1} \end{bmatrix}$. Then design sliding surface as

$$\sigma = \dot{e} + \mathcal{C}e \tag{34}$$

where $e = \mathfrak{X}_d - \mathfrak{X}_1$. Thus, the conventional SMC control law can be design as

$$u = \mathcal{G}^{-1}\left(-f + \ddot{\mathfrak{X}}_d + \mathcal{C}\dot{e} + \eta \mathrm{sgn}(\sigma)\right) \tag{35}$$

Then the adaptive SMC proposed in Zou et al. (2022) used RBFNN to approximate the dynamics f by

$$\widehat{f} = W_i^T H_i(X) + \varepsilon_i, W_i^T = \sigma h(x) \tag{36}$$

where $H_i(X) = [h_{i,1}(X), h_{i,2}(X), \cdots, h_{i,n}(X)]^T$ is same to equation (14). In such case, the adaptive SMC control law can be design as

$$u = \mathcal{G}^{-1}\left(-\widehat{f} + \ddot{\mathfrak{X}}_d + \mathcal{C}\dot{e} + \eta_1 \mathrm{sgn}(\sigma) + \eta_2 \sigma\right) \tag{37}$$

Table 2. SMC and adaptive SMC system design parameters.

Parameter	Value
$\mathcal{C}_1, \mathcal{C}_2$	5
η_1	5
b_j	5
η	5
η_2	5
$c_{i,j}$	$\begin{bmatrix} -1 & -0.5 & 0 & 0.5 & 1 \\ -1 & -0.5 & 0 & 0.5 & 1 \end{bmatrix}$

In the experimental simulation, the initial helicopter states are chosen as $\theta = \psi = 0$ and $\dot{\theta} = \dot{\psi} = 0$. The initial weights for RBFNN are set as $[0\,0\,0\,0\,0]$ with five nodes. $\theta_d = 0.2\sin(t)$ and $\psi_d = \pm\frac{\pi}{4}$ with 10 s change period are desired tracking attitude. The control inputs saturation is chosen as $u_{max} = 24$. The system external disturbances $d_i = 1$ are introduced into control inputs channels every 10 s for 3 s. The UDSMC control system framework is shown in Figure 6. The conventional SMC and adaptive SMC design parameters are presented in Table 2. The adaptive UDSMC system design parameters are provided in Table 3.

Remark 5. The problem of actuator saturation in practical engineering applications is to limit the actuator output to prevent the actuator from being overloaded and causing damage. This study also considers actuator saturation issue, which will affect system response and tracking control performance but will not affect controller stability.

Table 3. Adaptive UDSMC system design parameters.

Parameter	Value
c_1, c_2	5
$k_{sw,i}$	$5 + \lvert\mu_i\rvert$
b_j	5
ζ	1
ρ_i	10
δ_i	1
$k_{eq,i}$	5
$c_{i,j}$	$\begin{bmatrix} -1 & -0.5 & 0 & 0.5 & 1 \\ -1 & -0.5 & 0 & 0.5 & 1 \end{bmatrix}$
ω_n	1

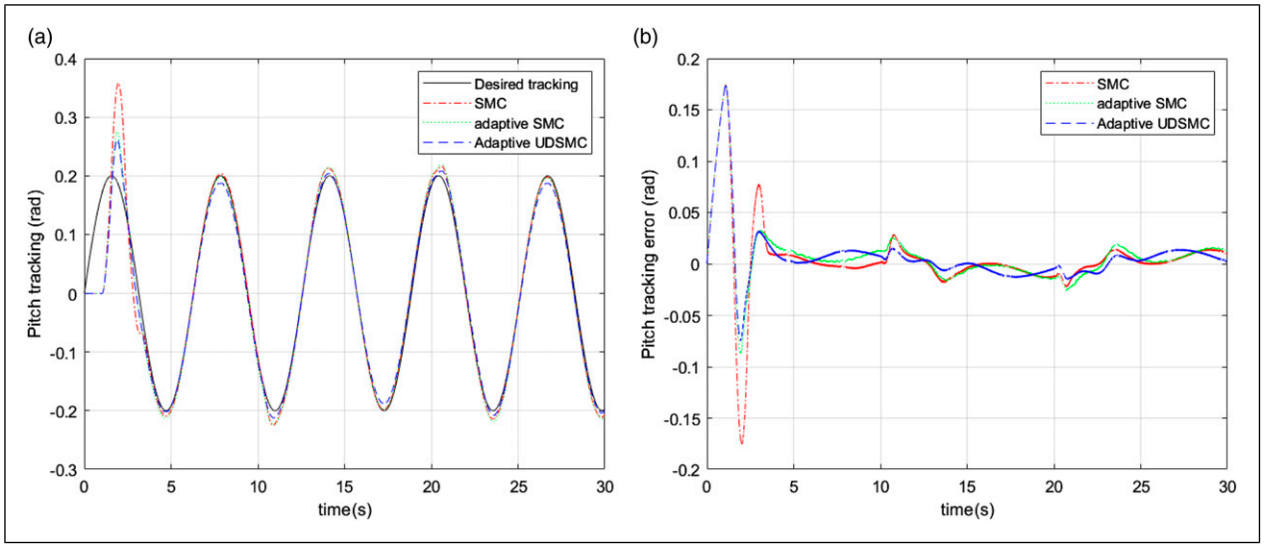

Figure 7. Pitch tracking comparison of SMC, adaptive SMC and adaptive UDSMC in Case 1 between (a) pitch angle tracking and (b) pitch tracking errors.

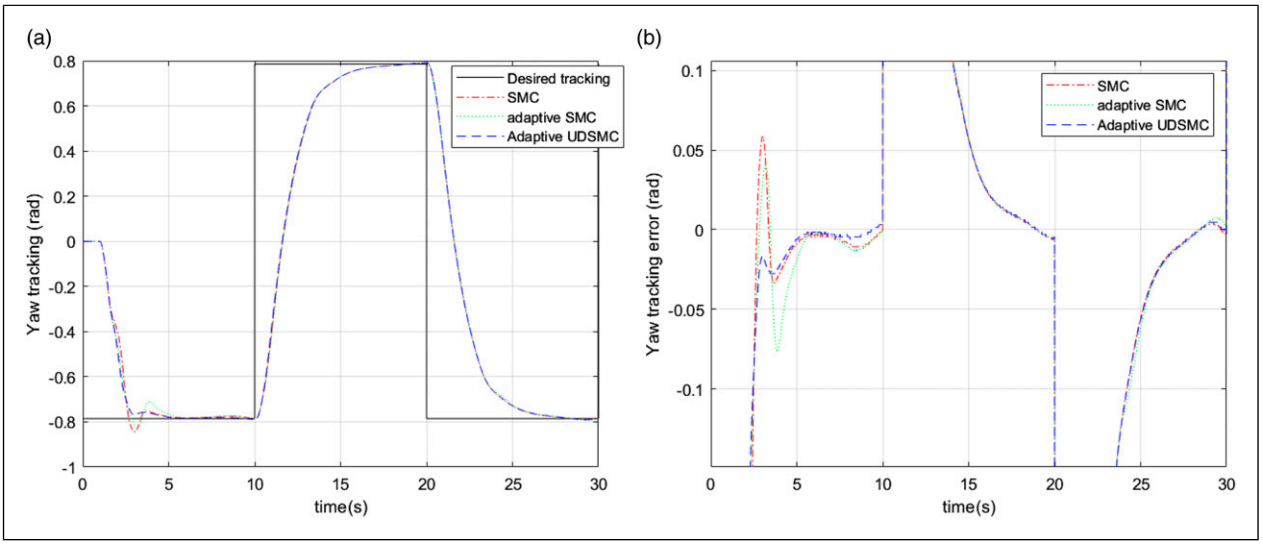

Figure 8. Yaw tracking comparison of SMC, adaptive SMC and adaptive UDSMC in Case 1 between (a) yaw angle tracking and (b) yaw tracking errors.

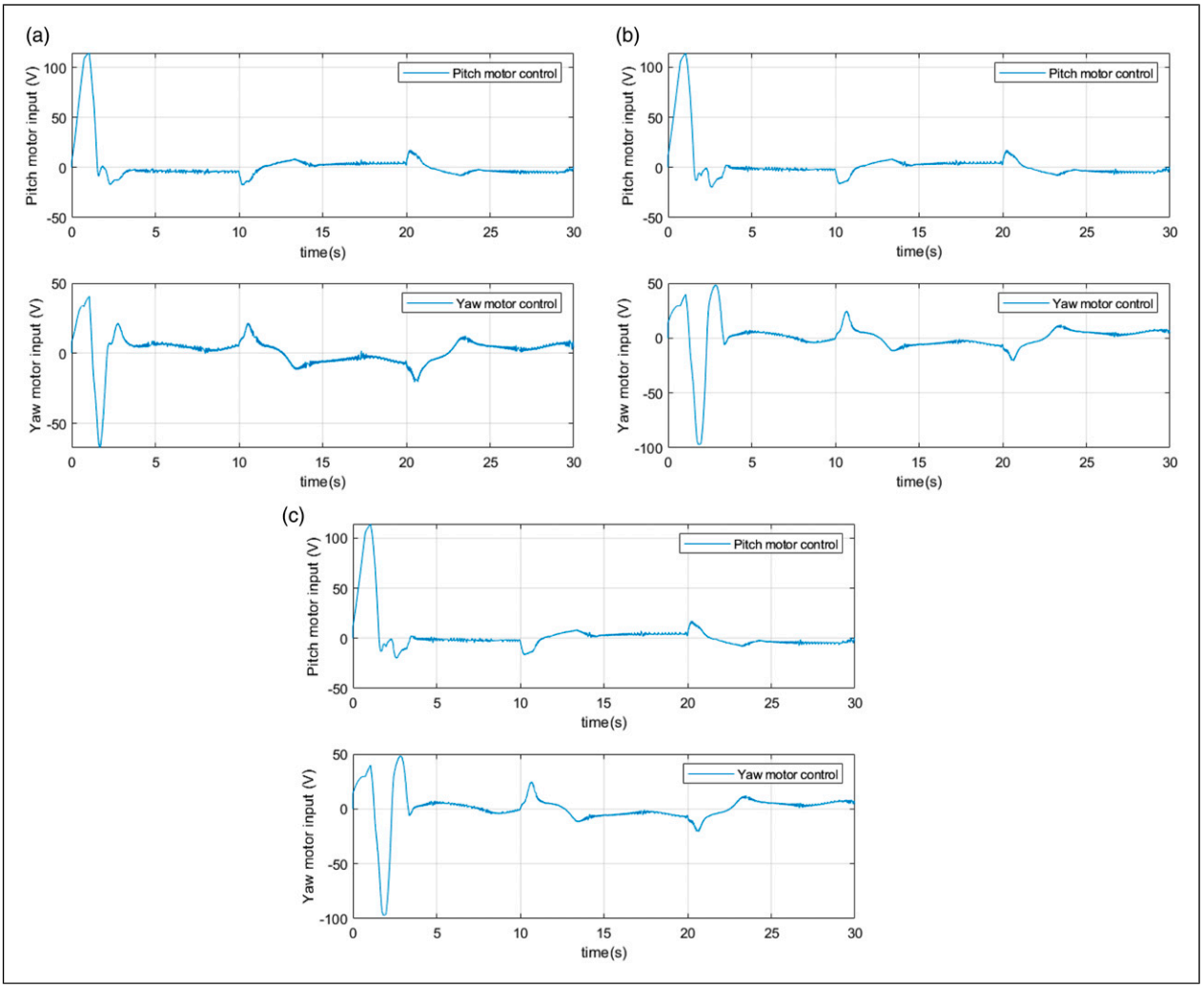

Figure 9. Comparison of control inputs in pitch and yaw motors in Case 1 between (a) SMC and (b) adaptive SMC and (c) adaptive UDSMC.

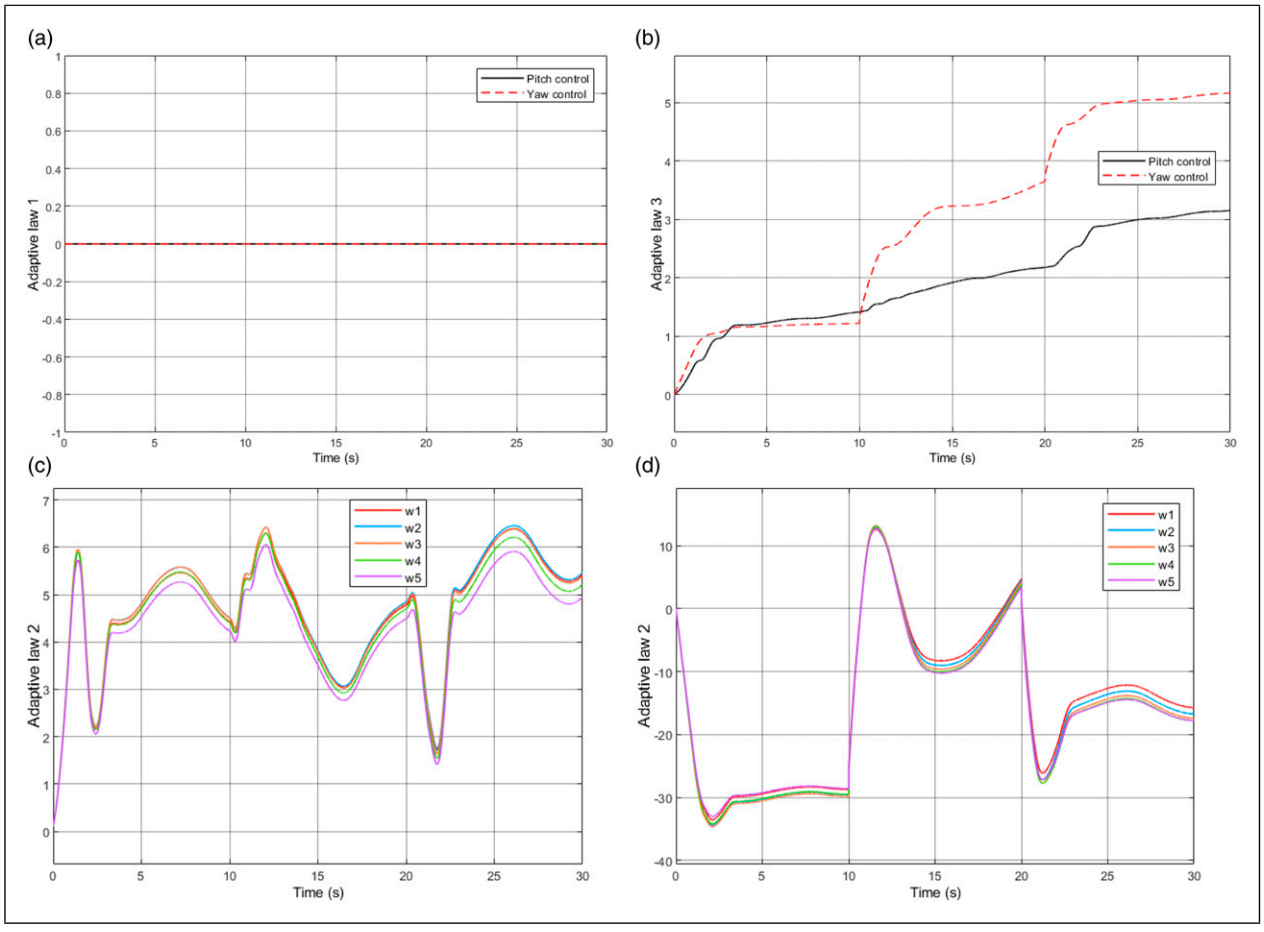

Figure 10. Comparison of adaptive UDSMC laws in pitch and yaw control in Case 1 between (a) adaptive law 1 in equation (16) and (b) adaptive law 3 in equation (22) and (c) adaptive law 2 in pitch control in equation (26) (d) adaptive law two in yaw control in equation (26).

4.1. Case 1: attitude tracking control

Figures 7–10 show the compared experimental results between the proposed adaptive UDSMC algorithm, SMC and adaptive SMC algorithms. In Figure 7, it can be observed that the adaptive UDSMC and adaptive SMC systems demonstrate better pitch angle tracking performance, exhibiting reduced overshoot and smaller tracking error. Similarly, in Figure 8, the adaptive UDSMC and adaptive SMC systems outperform the SMC system in terms of yaw angle tracking performance, showing decreased overshoot and smaller tracking error. From Figure 9, slight chattering can be observed from three SMC based control systems because unmodelled dynamics, helicopter mechanical vibration and sample period. Figure 10 shows the adaptive laws designed in adaptive UDSMC. Because Case 1 is free of control input saturation, adaptive law 1 equals 1, that is, has not been activated (from Figure 10(a)). Figure 10(c) and (d) show trends of adaptive law 2, which are weights for RBFNN. The adaptive law 2 varies with system following attitude and dynamics, therefore, the adaptive parameters in adaptive UDSMC are also adaptive.

To compare the tracking results for these three controllers numerically, the root mean square (RMS) values of the tracking errors are introduced as $e_{RMS} = \sqrt{\frac{1}{n}(e_1^2 + e_2^2 + \ldots + e_n^2)}$ with n being the total sampling size, the results are shown in Table 4. The control inputs numerical comparison results are calculated by the RMS ($u_{RMS} = \sqrt{\frac{1}{n}(u_1^2 + u_2^2 + \ldots + u_n^2)}$), and the results are shown in Table 5.

4.2. Case 2: attitude tracking control with input saturations and disturbances

In this experiment, external control input disturbances and control input saturation are introduced into comparative experiments to further verify the effectiveness of the proposed control system. Figure 11 shows the complex disturbance signal introduced to the input channel as voltage disturbance, which is predicted difficultly. Figures 12–15 show the compared experimental results between the proposed adaptive UDSMC algorithm, conventional SMC and

adaptive SMC (Zou et al., 2022) algorithms. From Figure 12, adaptive UDSMC system achieves better pitch angle tracking performance with less overshoot, smaller tracking error and fast convergence than both conventional SMC and adaptive SMC algorithms. Also, smaller overshoot in the initial sliding phase can be observed in adaptive UDSMC system from Figure 13 because of adaptive law 1 being introduced to compensate the error between desired control input and saturated control input. From Figure 14, three control systems could meet the control input saturation requirements. However, vigorous chattering issue can be observed from conventional SMC system because it cannot deal with control input saturation and unpredicted control input disturbance effectively. Also because of avoiding the overestimation of system uncertainties and disturbances, the proper input gain makes the average value of the input power of both adaptive SMC algorithms be smaller than that of SMC, which further reduces chattering problem. Figure 15 shows the adaptive laws designed in adaptive UDSMC for Case 2. Because Case 2 introduces control input saturation, adaptive law is activated to compensate control input error (from Figure 15(a)). Figure 15(c) and (d) show trends of adaptive law 2, which are weights for RBFNN design. Comparing with Figures 10 and 15, the adaptive law two varies with system following attitude and dynamics, therefore, the adaptive parameters in adaptive UDSMC are also adaptive.

Table 4. RMS results for trajectory tracking.

Channel	SMC	Adaptive SMC	Adaptive UDSMC
Pitch tracking error	0.0362	0.0303	0.0292
Yaw tracking error	0.4872	0.4869	0.4844

Table 5. RMS results for control inputs.

Channel	SMC	Adaptive SMC	Adaptive UDSMC
Pitch motor input	18.8076	18.7572	18.6772
Yaw motor input	16.7544	12.0701	11.8401

To compare the tracking results for these three controllers numerically, the RMS values of the tracking errors are shown in Table 6. The control inputs numerical comparison results are calculated by the RMS are shown in Table 7. Compare Table 4 with Table 6, control input saturation and input disturbance do have impact on control tracking performance. Comparing Table 5 with Table 6, two adaptive control system can save more energy than conventional SMC system because RBFNN can estimate unknown dynamics and then adjust control inputs synchronously.

4.3. *Case 3: attitude tracking control with input saturations, control input disturbances and wind.*

In this experiment, control input saturation, control input disturbances and external wind disturbances are introduced into comparative experiments to further verify the effectiveness of the proposed control system. The wind disturbance is introduced to system from 12 s to 20 s with

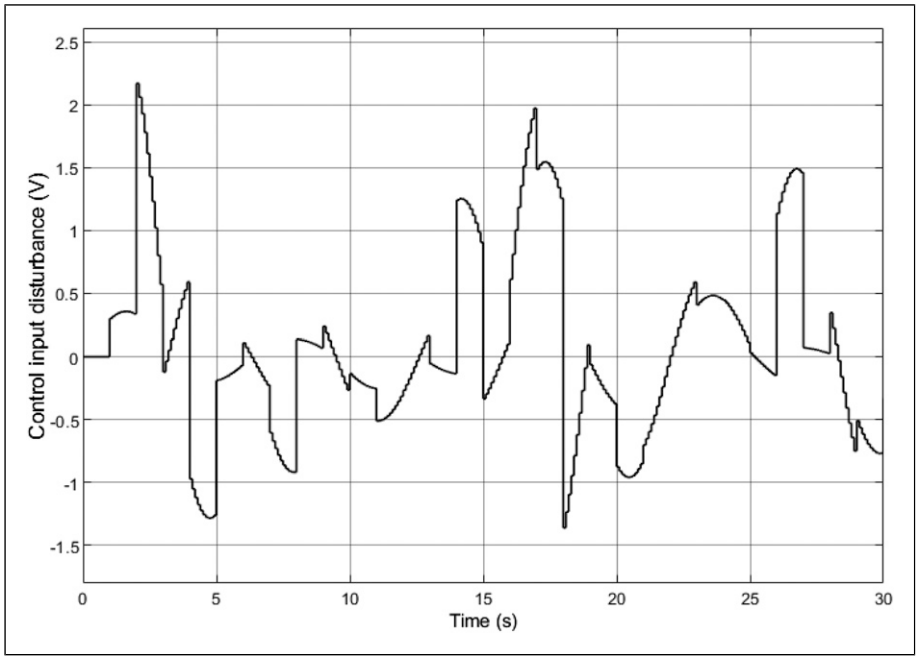

Figure 11. Disturbance introduced to input channel.

perpendicular direction of yaw motion. Figures 16–19 show the compared experimental results between the proposed adaptive UDSMC algorithm, conventional SMC and adaptive SMC (Zou et al., 2022) algorithms. From Figures 16 and 17, adaptive UDSMC system achieves better pitch and yaw angle tracking performance with less overshoot, smaller tracking error than both conventional SMC and adaptive SMC algorithms. Comparing with Figures 17 and 13, larger deviation in yaw tracking can be observed because of external wind disturbance. Also, smaller overshoot in the initial sliding phase can be observed in adaptive UDSMC system from Figure 17 because of adaptive law 1 being introduced to compensate the error between desired control input and saturated control input. From Figure 18, three control systems could meet the control input saturation requirements. However, vigorous chattering issue can be observed from conventional SMC system because it cannot deal with control input saturation and unpredicted control input disturbance effectively. Also, because of avoiding the overestimation of system uncertainties and disturbances, the proper input gain makes the average value of the input power of both adaptive SMC algorithms be smaller than that of SMC, which further reduces chattering problem. Figure 19 shows the adaptive laws designed in adaptive UDSMC. Because Case 3 also introduces control input saturation, adaptive law 1 is activated to compensate control input error

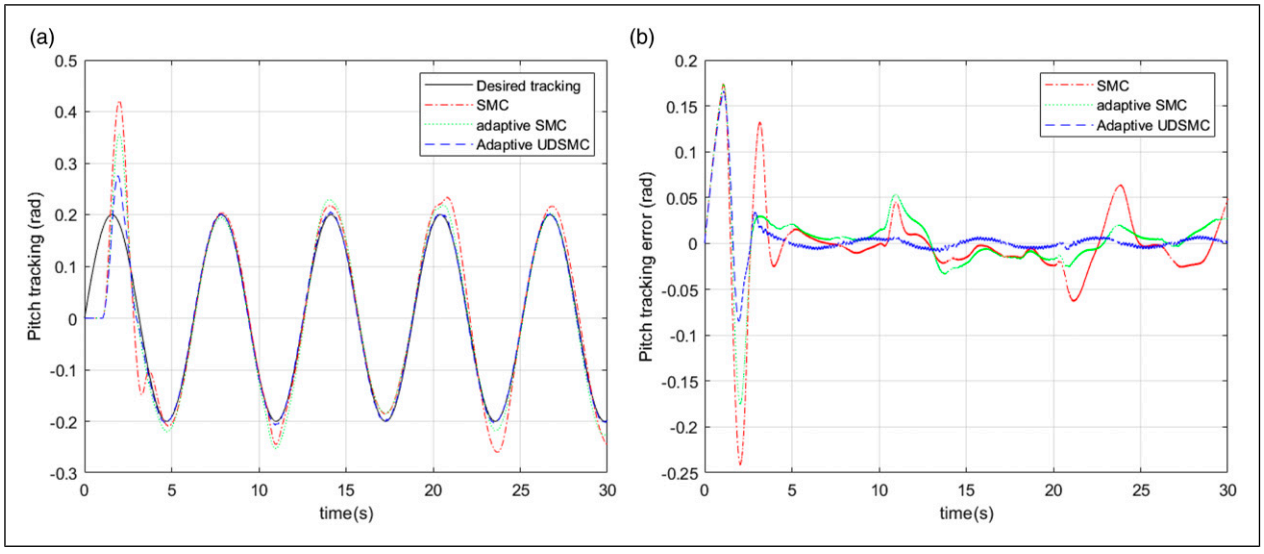

Figure 12. Pitch tracking comparison of SMC, adaptive SMC and adaptive UDSMC in Case 2 between (a) pitch angle tracking and (b) pitch tracking errors.

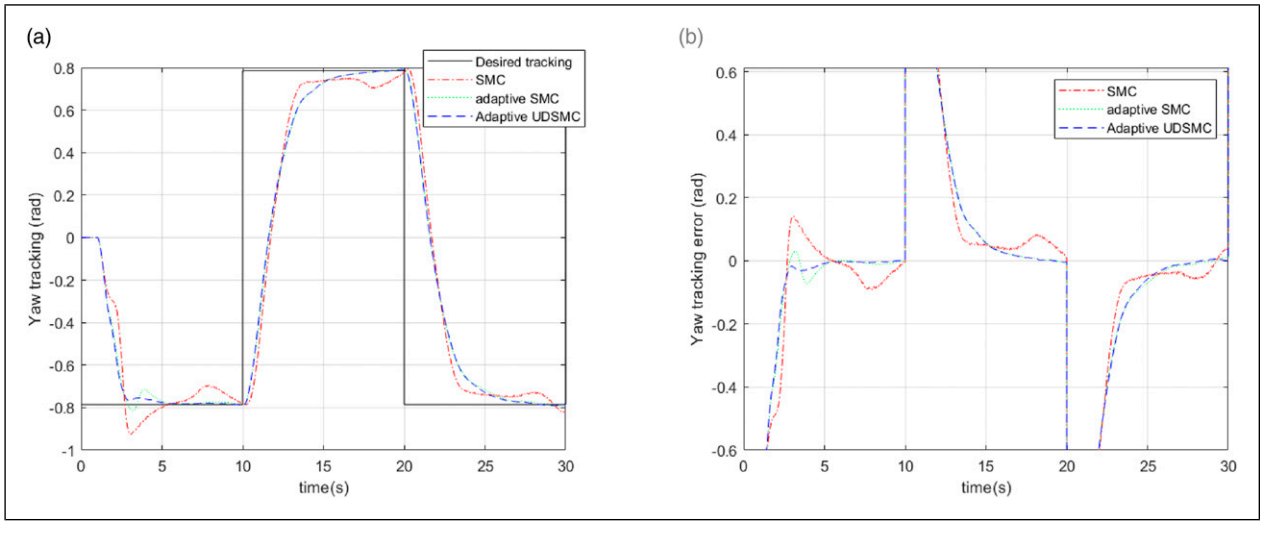

Figure 13. Yaw tracking comparison of SMC, adaptive SMC and adaptive UDSMC in Case 2 between (a) yaw angle tracking and (b) yaw tracking errors.

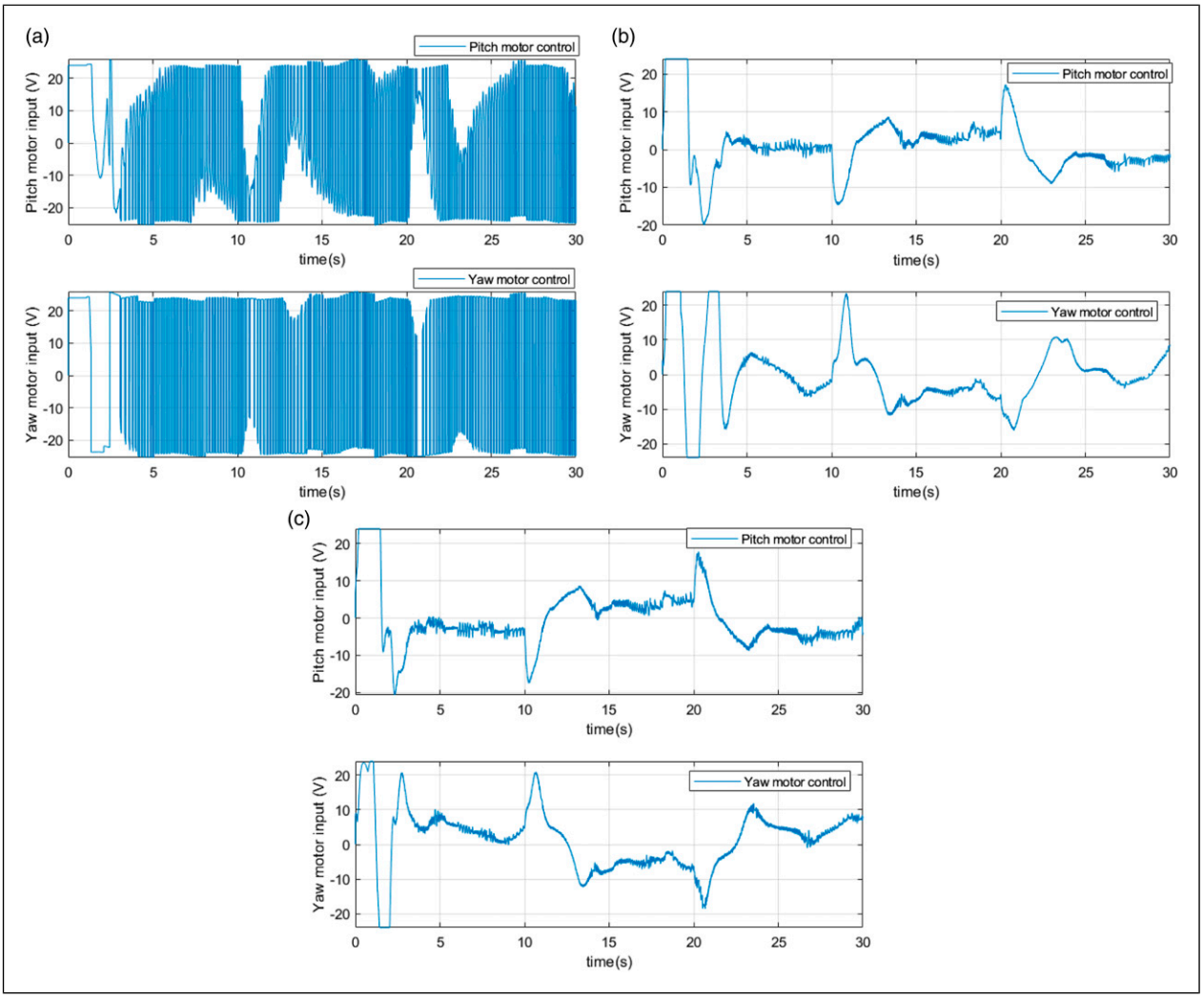

Figure 14. Comparison of control inputs in pitch and yaw motors in Case 2 between (a) SMC and (b) adaptive SMC and (c) adaptive UDSMC.

Table 6. RMS results for trajectory tracking.

Channel	SMC	Adaptive SMC	Adaptive UDSMC
Pitch tracking error	0.0493	0.0388	0.0292
Yaw tracking error	0.5109	0.4870	0.4844

Table 7. RMS results for control inputs.

Channel	SMC	Adaptive SMC	Adaptive UDSMC
Pitch motor input	19.9438	7.4541	7.6484
Yaw motor input	23.7296	9.3316	8.7959

(from Figure 19(a)). Figure 19(c) and (d) show trends of adaptive law 2, which are weights for RBFNN design. Comparing with Figures 10, 15 and 19, the adaptive law 1 and 2 varies with system following attitude and dynamics, therefore, the adaptive parameters in adaptive UDSMC are also adaptive (Figure 19).

To compare the tracking results for these three controllers numerically, the RMS values of the tracking errors

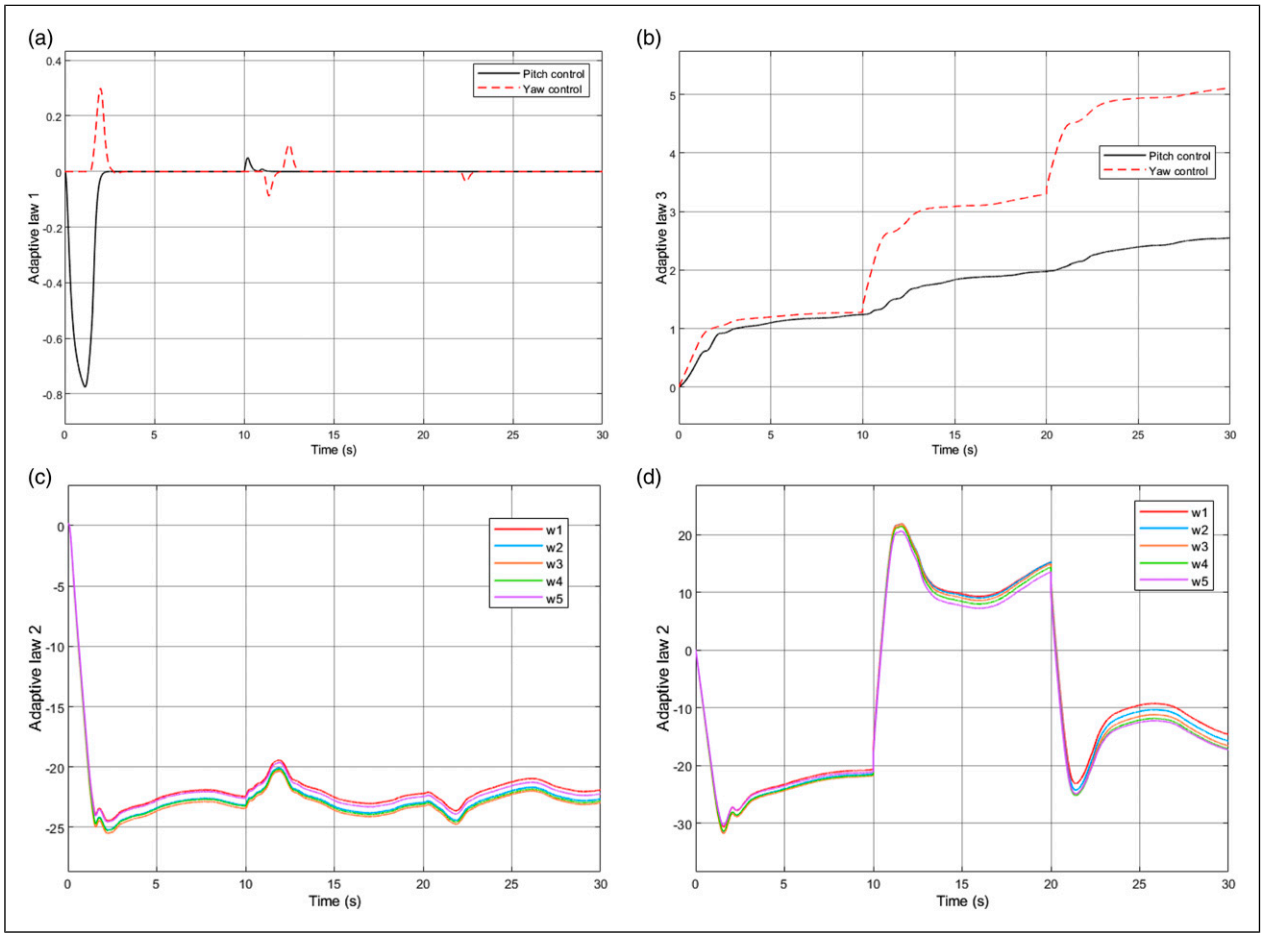

Figure 15. Comparison of adaptive UDSMC laws in pitch and yaw control in Case 2 between (a) adaptive law 1 in equation (16) and (b) adaptive law three in equation (22) and (c) adaptive law 2 in pitch control in equation (26) (d) adaptive law two in yaw control in equation (26).

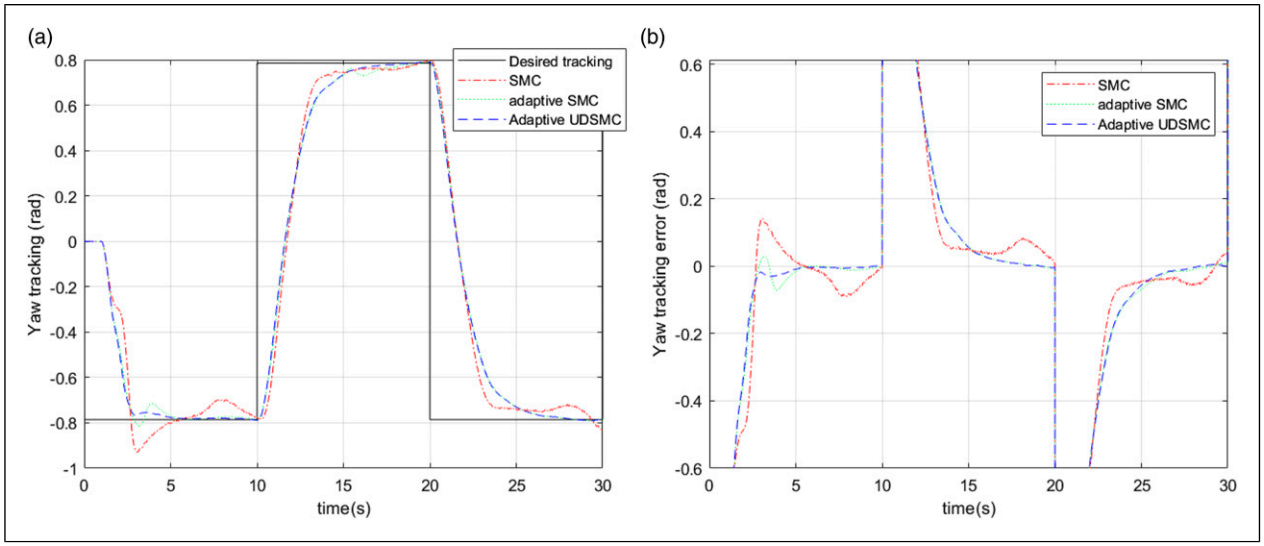

Figure 16. Pitch tracking comparison of SMC, adaptive SMC and adaptive UDSMC in Case 3 between (a) pitch angle tracking and (b) pitch tracking errors.

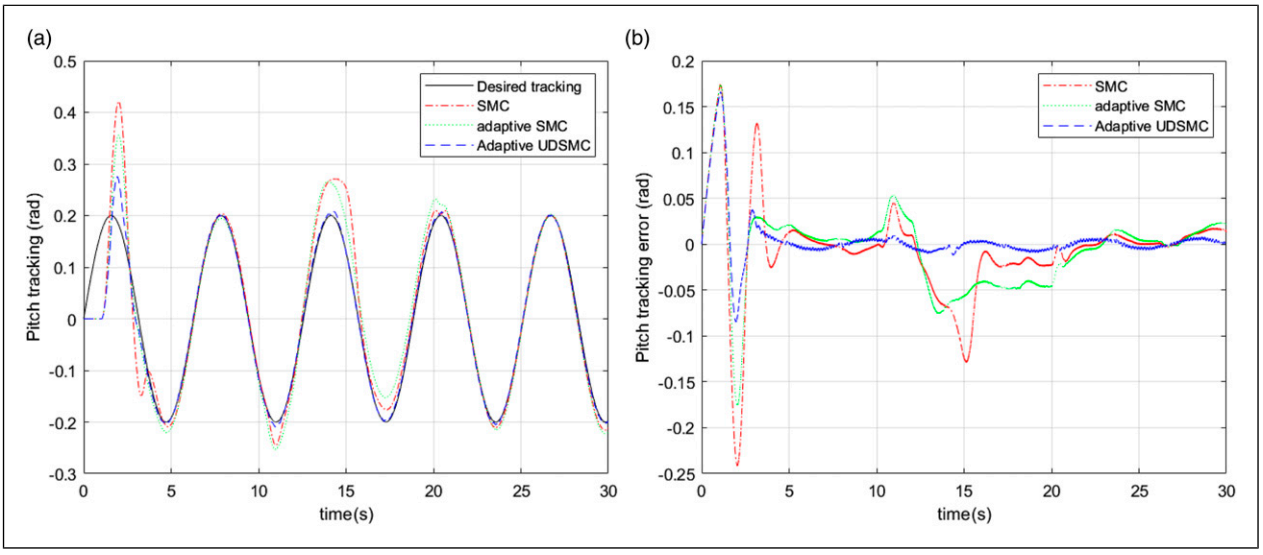

Figure 17. Yaw tracking comparison of SMC, adaptive SMC and adaptive UDSMC in Case 3 between (a) yaw angle tracking and (b) yaw tracking errors.

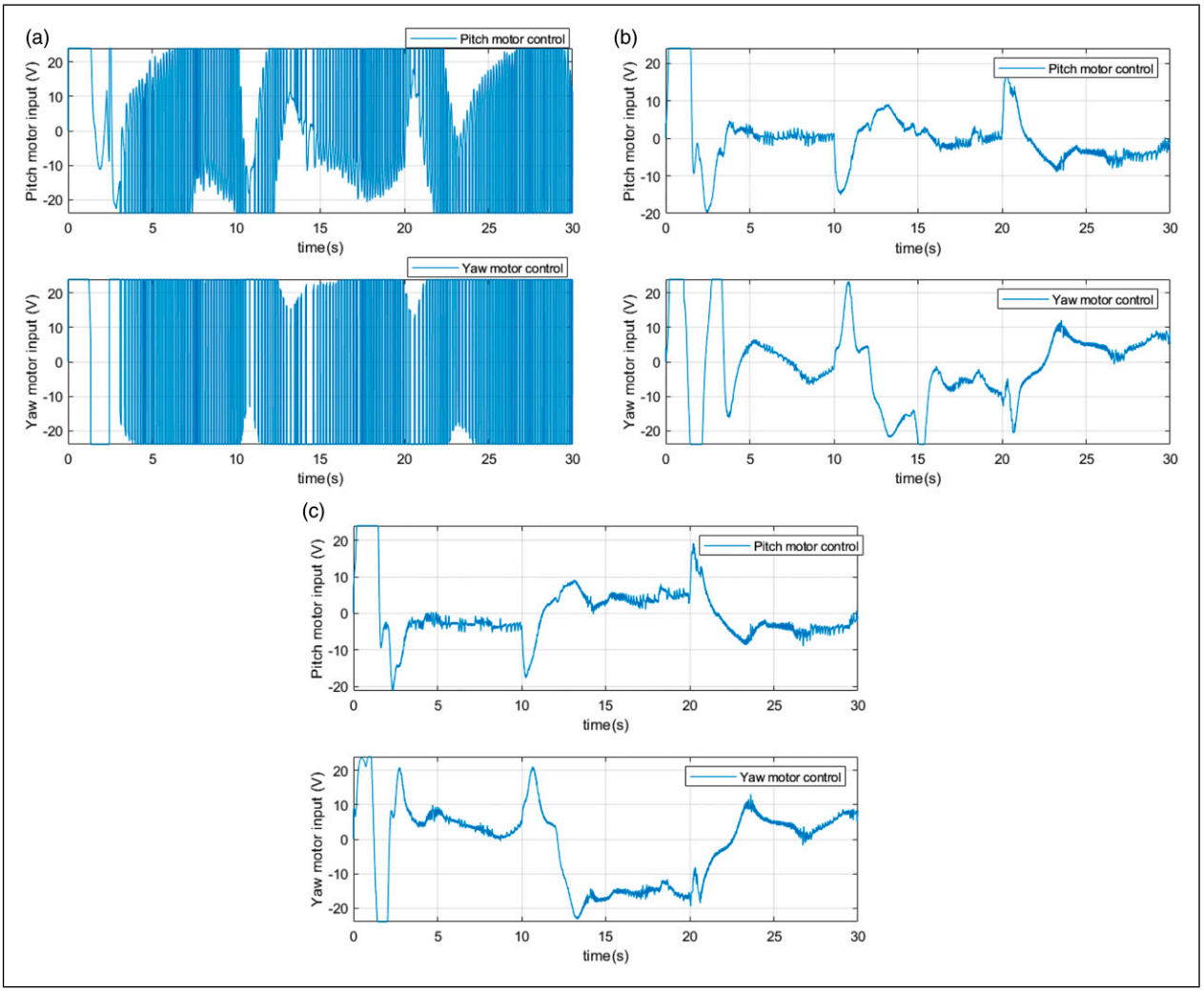

Figure 18. Comparison of control inputs in pitch and yaw motors in Case 3 between (a) SMC and (b) adaptive SMC and (c) adaptive UDSMC.

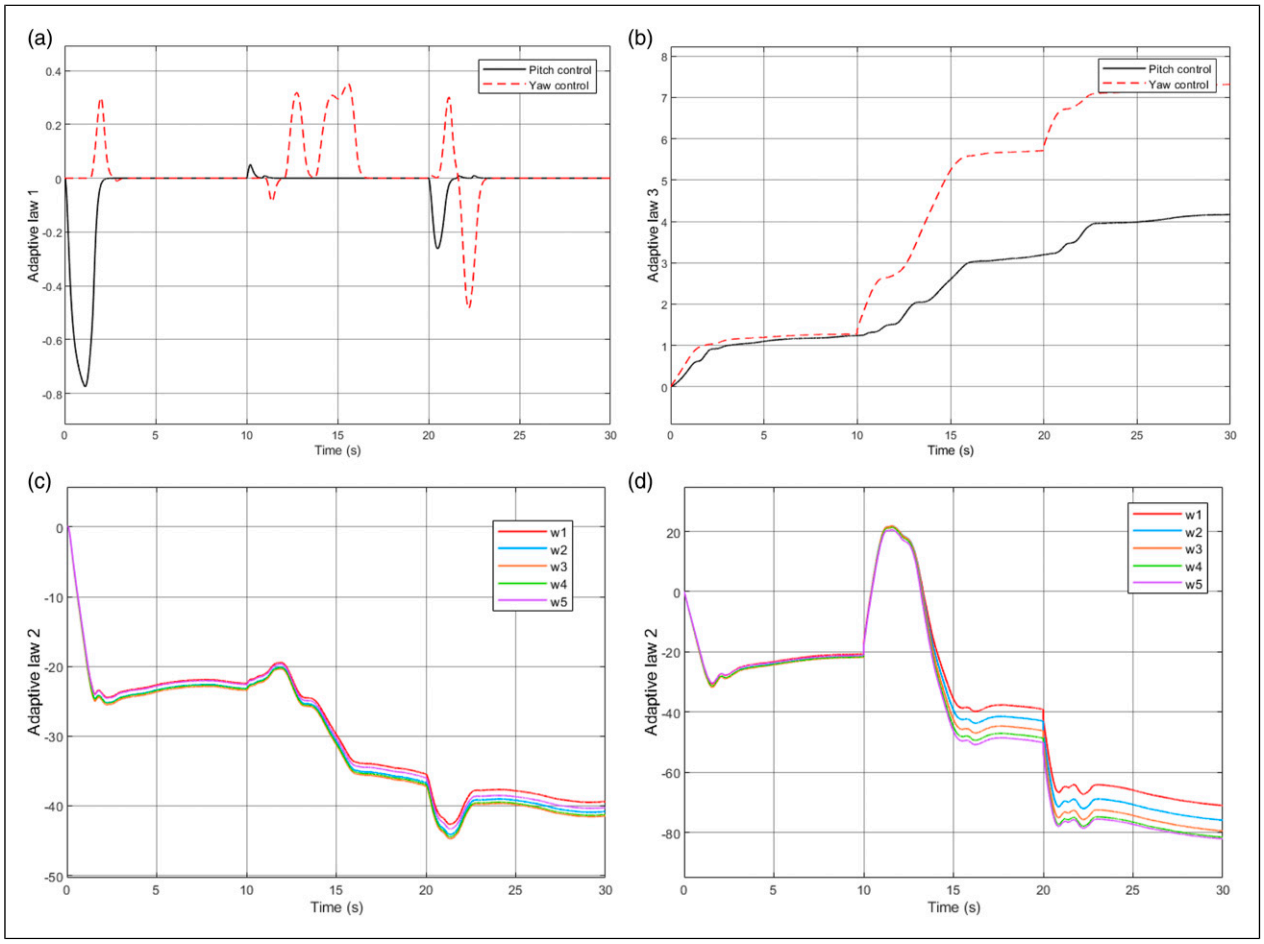

Figure 19. Comparison of adaptive UDSMC laws in pitch and yaw control in Case 3 between (a) adaptive law 1 in equation (16) and (b) adaptive law 3 in equation (22) and (c) adaptive law 2 in pitch control in equation (26) (d) adaptive law 2 in yaw control in equation (26).

Table 8. RMS results for trajectory tracking.

Channel	SMC	Adaptive SMC	Adaptive UDSMC
Pitch tracking error	0.0530	0.0455	0.0303
Yaw tracking error	0.5004	0.4872	0.4814

Table 9. RMS results for control inputs.

Channel	SMC	Adaptive SMC	Adaptive UDSMC
Pitch motor input	18.8681	7.4590	7.6961
Yaw motor input	23.7105	11.0389	11.6011

are shown in Table 8. The control inputs numerical comparison results are calculated by the RMS are shown in Table 9. Comparing Table 6 with Table 8, wind disturbance has more obvious impact on control tracking performance. Comparing Table 7 with Table 9, two adaptive control system can save more energy than conventional SMC system because RBFNN can estimate unknown dynamics and then adjust control inputs synchronously.

5. Conclusions

This study proposes an adaptive UDSMC control framework for a 2-DOF helicopter system with control input saturation, control input disturbance and external wind disturbance. The invariant controller can achieve specific control performance, the DSM inverter cancels the dynamics of the system and ensures the robustness, and the RBFNN is used to approximate the dynamics and uncertainties of the system. Combining them with the three adaptive laws allows the design of the proposed adaptive UDSMC without prior knowledge of the bounds of the external disturbances and precise parameters from 2-DOF helicopter model. The rigorous Lyapunov analysis was exploited to ensure system global asymptotic stability, achieving precise attitude tracking control of 2-DOF helicopter systems. Finally, comparative experimental results reveal the more feasible and effective control performance

of the proposed control algorithm compared with the conventional SMC and adaptive SMC.

However, the adaptive UDSMC associated with three adaptive laws presented in this study only considers convergence stability by using Lyapunov stability analysis, finite-time converge is not involved into this study. Therefore, our next research is trying to combine the finite-time SMC and finite-time RBFNN to establish a developed model-free/data-driven control system design framework.

Acknowledgements

The first author is acknowledging the partial PhD studentship for the research project and Quanser for providing Aero2 experimental platform.

Declaration of conflicting interests

The author(s) declared no potential conflicts of interest with respect to the research, authorship, and/or publication of this article.

Funding

The author(s) received no financial support for the research, authorship, and/or publication of this article.

ORCID iDs

Ruobing Li https://orcid.org/0000-0002-5154-007X
Quanmin Zhu https://orcid.org/0000-0001-8173-1179

References

Abiodun OI, Jantan A, Omolara AE, et al. (2018) State-of-the-art in artificial neural network applications: a survey. *Heliyon* 4(11): e00938.

Ahmed S, Azar AT and Tounsi M (2022a) Design of adaptive fractional-order fixed-time sliding mode control for robotic manipulators. *Entropy* 24(12): 1838.

Ahmed S, Ghous I and Mumtaz F (2022b) TDE based model-free control for rigid robotic manipulators under nonlinear friction. *Scientia Iranica* 19.

Bu X, Jiang B and Lei H (2022) Nonfragile quantitative prescribed performance control of waverider vehicles with actuator saturation. *IEEE Transactions on Aerospace and Electronic Systems* 58(4): 3538–3548.

Dong H, Yang X and Basin MV (2022) Practical tracking of permanent magnet linear motor via logarithmic sliding mode control. *IEEE/ASME Transactions on Mechatronics* 27(5): 4112–4121.

Fei J, Wang Z and Pan Q (2022) Self-constructing fuzzy neural fractional-order sliding mode control of active power filter. *IEEE Transactions on Neural Networks and Learning Systems* 1–12.

Feng Y, Han F and Yu X (2014) Chattering free full-order sliding-mode control. *Automatica* 50(4): 1310–1314.

Feng H, Song Q, Ma S, et al. (2022) A new adaptive sliding mode controller based on the RBF neural network for an electro-hydraulic servo system. *ISA Transactions* 129: 472–484.

Garcia RA, Rubio FR and Ortega MG (2012) Robust PID control of the quadrotor helicopter. *IFAC Proceedings Volumes* 45(3): 229–234.

Ghaffari V, Mobayen S, Ud Din S, et al. (2022) Robust tracking composite nonlinear feedback controller design for time-delay uncertain systems in the presence of input saturation. *ISA Transactions* 129: 88–99.

Guo G, Li P and Hao LY (2020) A new quadratic spacing policy and adaptive fault-tolerant platooning with actuator saturation. *IEEE Transactions on Intelligent Transportation Systems* 23(2): 1200–1212.

He W, Chen Y and Yin Z (2015) Adaptive neural network control of an uncertain robot with full-state constraints. *IEEE Transactions on Cybernetics* 46(3): 620–629.

Humaidi AJ and Hasan AF (2019) Particle swarm optimization–based adaptive super-twisting sliding mode control design for 2-degree-of-freedom helicopter. *Measurement and Control* 52(9–10): 1403–1419.

Inomoto RS, Monteiro JRBA and Filho AJS (2022) Boost converter control of PV system using sliding mode control with integrative sliding surface. *IEEE Journal of Emerging and Selected Topics in Power Electronics* 10(5): 5522–5530.

Kim SK and Ahn CK (2021) Performance-boosting attitude control for 2-DOF helicopter applications via surface stabilization approach. *IEEE Transactions on Industrial Electronics* 69(7): 7234–7243.

Kim BM and Yoo SJ (2021) Approximation-based quantized state feedback tracking of uncertain input-saturated MIMO nonlinear systems with application to 2-DOF helicopter. *Mathematics* 9(9): 1062.

Li Y and Lin Z (2018) *Stability and Performance of Control Systems with Actuator Saturation*. Boston: Birkhäuser.

Li R, Zhu Q, Kiely J, et al. (2020) Algorithms for U-model-based dynamic inversion (UM-dynamic inversion) for continuous time control systems. *Complexity* 2020: 1–14.

Li R, Zhu Q, Narayan P, et al. (2021a) U-model-based two-degree-of-freedom internal model control of nonlinear dynamic systems. *Entropy* 23(2): 169.

Li R, Zhu Q, Yang J, et al. (2021b) Disturbance-observer-based u-control (DOBUC) for nonlinear dynamic systems. *Entropy* 23(12): 1625.

Li R, Zhu Q, Zhang W, et al. (2022) An improved U-control design for nonlinear systems represented by input/output differential models with a disturbance observer. *International Journal of Control* 96: 2737–2748.

Li R, Zhu Q, Nemati H, et al. (2023) Trajectory tracking of a quadrotor using extend state observer based U-model enhanced double sliding mode control. *Journal of the Franklin Institute* 360(4): 3520–3544.

Milbradt DMC, Evald PJDO, Hollweg GV, et al. (2023) A hybrid robust adaptive sliding mode controller for partially modelled systems: discrete-time lyapunov stability analysis and application. *Nonlinear Analysis: Hybrid Systems* 48: 101333.

Mokhtari S, Abbaspour A, Yen KK, et al. (2021) Neural network-based active fault-tolerant control design for unmanned helicopter with additive faults. *Remote Sensing* 13(12): 2396.

Nkemdirim M, Dharan S, Chaoui H, et al. (2022) LQR control of a 3-DOF helicopter system. *International Journal of Dynamics and Control* 10: 1084–1093.

Reyhanoglu M, Jafari M and Rehan M (2022) Simple learning-based robust trajectory tracking control of a 2-DOF helicopter system. *Electronics* 11(13): 2075.

Sadala SP and Patre BM (2018) A new continuous sliding mode control approach with actuator saturation for control of 2-DOF helicopter system. *ISA Transactions* 74: 165–174.

Shao K, Zheng J, Tang R, et al. (2022) Barrier function based adaptive sliding mode control for uncertain systems with input saturation. *IEEE/ASME Transactions on Mechatronics* 27(6): 4258–4268.

Shen S and Xu J (2021) Adaptive neural network-based active disturbance rejection flight control of an unmanned helicopter. *Aerospace Science and Technology* 119: 107062.

Shtessel Y and Edwards C (2014) *Sliding Mode Control and Observation*. New York: Springer, Vol. 10.

Son NN, Van Kien C and Anh HPH (2022) Adaptive sliding mode control with hysteresis compensation-based neuroevolution for motion tracking of piezoelectric actuator. *Applied Soft Computing* 115: 108257.

Soon CC, Ghazali R, Ghani MF, et al. (2022) Chattering analysis of an optimized sliding mode controller for an electro-hydraulic actuator system. *Journal of Robotics and Control (JRC)* 3(2): 160–165.

Utkin V, Guldner J and Shi J (2017) *Sliding Mode Control in Electro-Mechanical Systems*. Boca Raton, FL: CRC Press.

Wan S, Li X, Su W, et al. (2020) Active chatter suppression for milling process with sliding mode control and electromagnetic actuator. *Mechanical Systems and Signal Processing* 136: 106528.

Wang B, Shen Y and Zhang Y (2020) Active fault-tolerant control for a quadrotor helicopter against actuator faults and model uncertainties. *Aerospace Science and Technology* 99: 105745.

Wu B, Wu J, He W, et al. (2022a) Adaptive neural control for an uncertain 2-DOF helicopter system with unknown control direction and actuator faults. *Mathematics* 10(22): 4342.

Wu Z, Wang Q and Huang H (2022b) Adaptive neural networks trajectory tracking control for autonomous underwater helicopters with prescribed performance. *Ocean Engineering* 264: 112519.

Wu B, Wu J, Zhang J, et al. (2022c) Adaptive neural control of a 2DOF helicopter with input saturation and time-varying output constraint. *Actuators* 11(11): 336.

Yang Y and Niu Y (2023) Co-design of scheduling protocol and fuzzy sliding mode controller under communication constraints. *Automatica* 147: 110698.

Ye Z, Zhang D, Cheng J, et al. (2022) Event-triggering and quantized sliding mode control of UMV systems under DoS attack. *IEEE Transactions on Vehicular Technology* 71(8): 8199–8211.

Zhang Q, Song X, Song S, et al. (2023) Finite-time sliding mode control for singularly perturbed PDE systems. *Journal of the Franklin Institute* 360(2): 841–861.

Zhang X and Xian B (2021) Attitude control for an unmanned helicopter using passivity-based iterative learning. In: 40th Chinese control conference (CCC), Shanghai, China, 26–28 July 2021, pp. 2127-2132. IEEE.

Zhao Z, He W, Mu C, et al. (2022a) Reinforcement learning control for a 2-DOF helicopter with state constraints: theory and experiments. *IEEE Transactions on Automation Science and Engineering* 1–11.

Zhao Z, Zhang J, Liu Z, et al. (2022b) *Adaptive neural network control of an uncertain 2-DOF helicopter with unknown backlash-like hysteresis and output constraints*. Piscataway, NY: IEEE Transactions on Neural Networks and Learning Systems, pp. 1–10.

Zhu Z, Xia Y and Fu M (2011) Adaptive sliding mode control for attitude stabilization with actuator saturation. *IEEE Transactions on Industrial Electronics* 58(10): 4898–4907.

Zhu Q, Li R and Yan X (2022) U-model-based double sliding mode control (UDSM-control) of nonlinear dynamic systems. *International Journal of Systems Science* 53(6): 1153–1169.

Zhu G, Ma Y and Hu S (2023) Event-triggered adaptive PID fault-tolerant control of underactuated ASVs under saturation constraint. *IEEE Transactions on Systems Man and Cybernetics: Systems* 53: 4922–4933.

Zou T, Wu H, Sun W, et al. (2022) Adaptive neural network sliding mode control of a nonlinear two-degrees-of-freedom helicopter system. *Asian Journal of Control* 25: 2085–2094.